

# How water contributes to pressure and cold denaturation of proteins

Valentino Bianco, Giancarlo Franzese

December 24, 2018

Departament de Física Fonamental, Universitat de Barcelona, Martí i Franquès 1, 08028 Barcelona, Spain

gfranzese@ub.edu

## Abstract

The mechanisms of cold- and pressure-denaturation of proteins are matter of debate and are commonly understood as due to water-mediated interactions. Here we study several cases of proteins, with or without a unique native state, with or without hydrophilic residues, by means of a coarse-grain protein model in explicit solvent. We show, using Monte Carlo simulations, that taking into account how water at the protein interface changes its hydrogen bond properties and its density fluctuations is enough to predict protein stability regions with elliptic shapes in the temperature-pressure plane, consistent with previous theories. Our results clearly identify the different mechanisms with which water participates to denaturation and open the perspective to develop advanced computational design tools for protein engineering.

PACS number 87.15.Cc, 87.15.A-, 87.15.kr.

Water plays an essential role in driving the folding of a protein and in stabilizing the tertiary protein structure in its native state [1, 2]. Proteins can denature—unfolding their structure and losing their activity—as a consequence of changes in the environmental conditions. Experimental data show that for many proteins the native folded state is stable in a limited range of temperatures  $T$  and pressures  $P$  [3, 4, 5, 6, 7, 8] and that partial folding is  $T$ -modulated also in “intrinsically disordered proteins” [9]. By hypothesizing that proteins have only two different states, folded ( $f$ ) and unfolded ( $u$ ), and that the  $f \longleftrightarrow u$  process is reversible at any moment, Hawley proposed a theory [10] that predicts a close stability region (SR) with an elliptic shape in the  $T - P$  plane, consistent with the experimental data [11].

Cold- and pressure-denaturation of proteins have been related to the equilibrium properties of the hydration water [12, 13, 14, 15, 16, 17, 18, 19, 20, 21, 22, 23]. However, the interpretations of the mechanism is still controversial [24, 25, 26, 27, 28, 29, 8, 30, 31]. High- $T$  denaturation is easily understood in terms of thermal fluctuations that disrupt the compact protein conformation: the open protein structure increases the entropy  $S$  minimizing the global Gibbs free energy  $G \equiv H - TS$ , where  $H$  is the total enthalpy. Cold- and pressure-unfolding can be thermodynamically justified assuming an enthalpic gain of the solvent upon denaturation process, without specifying the origin of this gain from molecular interactions [32]. Here, we propose a molecular-interactions model for proteins solvated by explicit water, based on the “many-body” water model [33, 34, 35, 36, 29, 37]. We demonstrate how the cold- and pressure-denaturation mechanisms emerge as a competition between different free energy contributions coming from water, one from hydration water and another from bulk water. Moreover, we show how changes in

the protein sequence affect the hydration water properties and, in turn, the stability of the protein folded state—a relevant information in protein design [25].

The many-body water model adopts a coarse-grain (CG) representation of the water coordinates by partitioning the available volume  $V$  into a fixed number  $N_0$  of cells, each with volume  $v \equiv V/N_0 \geq v_0$ , where  $v_0$  is the water excluded volume. Each cell accommodates at most one molecule with the average O–O distance between next neighbor (n.n.) water molecules given by  $r = v^{1/3}$ . To each cell we associate a variable  $n_i = 1$  if the cell  $i$  is occupied by a water molecule and has  $v_0/v > 0.5$ , and  $n_i = 0$  otherwise. Hence,  $n_i$  is a discretized density field replacing the water translational degrees of freedom. The Hamiltonian of the bulk water

$$\mathcal{H} \equiv \sum_{ij} U(r_{ij}) - JN_{\text{HB}}^{(\text{b})} - J_{\sigma}N_{\text{coop}} \quad (1)$$

has a first term, summed over all the water molecules  $i$  and  $j$  at O–O distance  $r_{ij}$ , accounting for the van der Waals interaction, with  $U(r) \equiv \infty$  for  $r < r_0 \equiv v_0^{1/3} = 2.9 \text{ \AA}$  (water van der Waals diameter),  $U(r) \equiv 4\epsilon[(r_0/r)^{12} - (r_0/r)^6]$  for  $r \geq r_0$  with  $4\epsilon \equiv 5.8 \text{ kJ/mol}$  and  $U(r) \equiv 0$  for  $r > r_c \equiv 6r_0$  (cutoff).

The second term represents the directional (covalent) component of the hydrogen bond (HB), with  $J/4\epsilon = 0.3$  [38],  $N_{\text{HB}}^{(\text{b})} \equiv \sum_{\langle ij \rangle} n_i n_j \delta_{\sigma_{ij}, \sigma_{ji}}$  number of bulk HBs, with the sum over n.n., where  $\sigma_{ij} = 1, \dots, q$  is the bonding index of molecule  $i$  to the n.n. molecule  $j$ , with  $\delta_{ab} = 1$  if  $a = b$ , 0 otherwise. Each water molecule can form up to four HBs that break if  $n_i n_j = 0$ , i.e.  $r_{ij} > 2^{1/3}r_0 = 3.6 \text{ \AA}$ , or  $\widehat{\text{OOH}} > 30^\circ$ . Hence, only 1/6 of the entire range of values  $[0, 360^\circ]$  for the  $\widehat{\text{OOH}}$  angle is associated to a bonded state. Therefore, we choose  $q = 6$  to account correctly for the entropy variation due to the HB formation and breaking.

The third term accounts for the HB cooperativity due to the quantum many-body interaction [39], with  $J_{\sigma}/4\epsilon \equiv 0.05$  and  $N_{\text{coop}} \equiv \sum_i n_i \sum_{(l,k)_i} \delta_{\sigma_{ik}, \sigma_{il}}$ , where  $(l, k)_i$  indicates each of the six different pairs of the four indices  $\sigma_{ij}$  of a molecule  $i$ . The value  $J_{\sigma} \ll J$  is chosen in such a way to guarantee an asymmetry between the two components of the HB interaction. This term is due the O–O–O correlation that locally leads the molecules toward a tetrahedral structure (all variables  $\sigma$  in the same bonding state), consistent with experiments at low  $P$  up to the second shell [40].

Increasing  $P$  partially disrupts the open structure of the HB network and reduces  $v$  toward  $v_0$ . We account for this with an average enthalpy increase  $Pv_{\text{HB}}^{(\text{b})}$  per HB, where  $v_{\text{HB}}^{(\text{b})}/v_0 = 0.5$  is the average volume increase between high- $\rho$  ices VI and VIII and low- $\rho$  (tetrahedral) ice Ih. Hence, the total bulk volume is

$$V^{(\text{b})} \equiv Nv_0 + N_{\text{HB}}^{(\text{b})}v_{\text{HB}}^{(\text{b})}. \quad (2)$$

We assume that the HBs do not affect the n.n. distance  $r$ , consistent with experiments [40], hence do not affect the  $U(r)$  term.

Next we consider the effect of the protein interface on the hydration water. First we consider water near a hydrophobic ( $\Phi$ ) residue. Experiments and atomistic simulations provide evidences that in this case water-water HBs are more stable than in bulk [41, 42, 43] with stronger water-water correlation [44]. This can be modeled by assuming that for HBs at the  $\Phi$  interface the covalent energy  $J$  of Eq. (1) is replaced by  $J_{\Phi} > J$ . This choice, according to the Muller discussion [32], ensures the water enthalpy compensation during the cold-denaturation [45].

The presence of the  $\Phi$  interface affects the hydration water density and fluctuations. The effect has been debated, with some works suggesting a decrease of hydration water density [46, 47, 48, 49], while more recent simulations have shown an increase of density in the first hydration shell of any solute [50] and an increase of compressibility near  $\Phi$  solutes with size  $\gtrsim 0.5 \text{ nm}$  for water [51, 44, 26] or water-like solvents [52] with respect to bulk. Increasing  $P$  induces an increase of density and reduces the compressibility of the hydration shell [44, 26]. This effect can be incorporated into the model by using the following thermodynamic considerations. From the equilibrium condition for the thermodynamic potential of hydration water and the coexisting vapor at the  $\Phi$  interface at fixed  $T$ , according to the Eq.

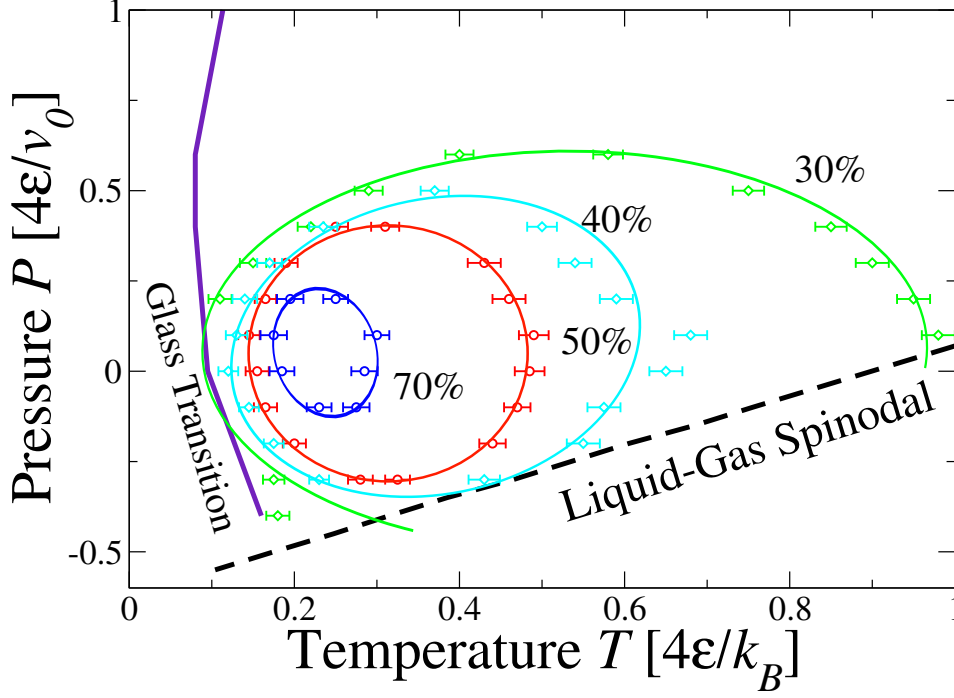


Figure 1: Stability region (SR) of the protein from Monte Carlo simulations in the  $P-T$  plane. Symbols connected by lines mark state points with the same average residue-residue contact's number  $n_{\text{tr}}/n_{\text{max}} = 30\%$ ,  $40\%$ ,  $50\%$  and  $70\%$ . Elliptic lines are guides for the eyes. The “glass transition” line defines the temperatures below which the system does not reach equilibrium. The spinodal line marks the stability limit of the liquid phase at high  $P$  with respect to the gas at low  $P$ . Here  $k_B$  is the Boltzmann constant.

(2) of Ref. [53], we deduce  $v^{(\Phi)} - v_0 \sim (P - P^*)^{-1}$ , where  $v^{(\Phi)}$  is the volume per hydration water molecule and  $P^* < 0$  is the equilibrium vapor pressure at the given  $T$ . If we attribute this  $P$ -dependence to the interfacial HB properties ( $v_{\text{HB}}^{(\Phi)} \sim v^{(\Phi)} - v_0$ ) and expand it as a power series in  $P$ , the average volume change per water-water HB at the  $\Phi$  interface is

$$v_{\text{HB}}^{(\Phi)}/v_{\text{HB},0}^{(\Phi)} \equiv 1 - k_1 P + k_2 P^2 - k_3 P^3 + O(P^4) \quad (3)$$

where  $v_{\text{HB},0}^{(\Phi)}$  is the volume change associated to the HB formation in the  $\Phi$  hydration shell at  $P = 0$ ,  $k_i > 0 \forall i$  and  $\lim_{P \rightarrow \infty} v_{\text{HB}}^{(\Phi)} = 0$ . Hence, the total volume  $V$  is

$$V \equiv V^{(\text{b})} + V^{(\Phi)} \equiv V^{(\text{b})} + N_{\text{HB}}^{(\Phi)} v_{\text{HB}}^{(\Phi)}, \quad (4)$$

where  $V^{(\Phi)}$  and  $N_{\text{HB}}^{(\Phi)}$  are the  $\Phi$  hydration shell volume and number of HBs, respectively.

Because we are interested to small values of  $P$ , i.e. near the biologically relevant atmospheric pressure, we include in our calculations only the linear term in Eq.(3) [54]. We do not observe qualitatively changes in our results by including up to the third order in Eq.(3). In the following we fix  $k_1 = 1v_0/4\epsilon$ ,  $v_{\text{HB},0}^{(\Phi)}/v_0 = v_{\text{HB}}^{(\text{b})}/v_0 = 0.5$  and  $J_{\Phi}/J = 1.83$ .

Because our goal here is to calculate the water contribution to denaturation, we model the protein as a self-avoiding  $\Phi$  homopolymer whose residues occupy n.n. cells with no residue-residue interaction but

the excluded volume, as in other CG approaches to the  $f \longleftrightarrow u$  process [15, 55, 16, 18]. This implies that the protein has several “native” states, all with the same maximum number  $n_{\max}$  of residue-residue contacts.

We analyze the system by Monte Carlo simulations at constant  $N, P, T$ . We adopt a representation in two dimensions (2D) [15, 16, 18, 56, 12], using a square partition, to favor visualization and qualitative understanding of our results. Comparisons with our preliminary results in 3D do not show qualitative changes, mainly because the number of n.n. water molecules is four both in 2D and 3D for the tendency of water to form tetrahedral structures in 3D.

We consider that the protein is folded if the average number of residue-residue contacts  $n_{\text{rr}} \geq 50\% n_{\max}$ . We find an elliptic SR (Fig.1), consistent with experiments and the Hawley theory [10, 11], with heat-, cold-, and pressure-unfolding. The elliptic shape is preserved when we change the threshold of number of residue-residue contacts, showing that the  $f \longleftrightarrow u$  is a continuous process. In the SR the folded protein (Fig. 2a) is stabilized by minimizing the number of  $\Phi$  residues exposed to water, reducing the energy cost of the interface, as expected.

First, we observe that the model reproduces the expected *entropy-driven*  $f \longleftrightarrow u$  for increasing  $T$  at constant  $P$  (Fig. 2b). The entropy  $S$  increases both for the opening of the protein and for the larger decrease of  $N_{\text{HB}}^{(\text{b})}$  and  $N_{\text{HB}}^{(\Phi)}$ .

Next, we focus on how water contributes to the cold denaturation (Fig. 2c). Upon isobaric decrease of  $T$  the internal energy dominates the system Gibbs free energy. However,  $N_{\text{HB}}^{(\text{b})}$  saturates at  $T$  lower than the SR, therefore the only way for the system to further minimize the internal energy is to increase  $N_{\text{HB}}^{(\Phi)}$ , i.e. to unfold the protein. Hence, the cold denaturation is an *energy-driven* process toward a protein state that is stabilized by the increased number of HBs in the hydration shell.

Next, upon isothermal increase of  $P$  the protein denaturates for pressurization (Fig. 2d), with decrease of  $N_{\text{HB}}^{(\text{b})}$  and small increase of  $N_{\text{HB}}^{(\Phi)}$ , resulting in an increase of the internal energy. However, the changes of  $N_{\text{HB}}^{(\text{b})}$  and  $N_{\text{HB}}^{(\Phi)}$  imply a decrease of volume, Eq. (4), leading to a minimization of  $PV$  that, at high  $P$ , is large enough to minimize the entire Gibbs free energy. Therefore, the high- $P$  denaturation is *density-driven*, as emphasized by the large increase of local density near the unfolded protein (Fig. 2d).

Finally, upon isothermal decrease of  $P$  toward negative values (Fig. 2e), the enthalpy decreases when the contribution  $(Pv_{\text{HB}}^{(\Phi)} - J_{\Phi})N_{\text{HB}}^{(\Phi)}$  decreases, i.e. when  $N_{\text{HB}}^{(\Phi)}$  increases. Therefore, we find that under depressurization the denaturation process is *enthalpy-driven*.

From the Clapeyron relation  $dP/dT = \Delta S/\Delta V$  applied to the SR [10], we expect that the  $f \longleftrightarrow u$  process is isochoric at the SR turning points where  $\partial T/\partial P|_{\text{SR}} = 0$ , while is isoentropic at the turning points where  $\partial P/\partial T|_{\text{SR}} = 0$ . In particular, at any  $T$  and  $P$  the volume change in the  $f \longrightarrow u$  process is given by

$$\Delta V \equiv V_u - V_f \simeq v_{\text{HB}}^{(\text{b})}\Delta N_{\text{HB}}^{(\text{b})} + (v_{\text{HB},0}^{(\Phi)} - k_1 P)\Delta N_{\text{HB}}^{(\Phi)}. \quad (5)$$

We estimate the Eq. (5) calculating the average volume  $V_u$  and  $V_f$  in a wide range of  $T$  and  $P$ , equilibrating water around a completely unfolded protein state and a completely folded state (with  $n_{\text{rr}} = n_{\max}$ ). Consistently with the Hawley’s theory [10], we find that the  $P$ -denaturation is accompanied by a decrease of volume  $\Delta V < 0$  at high  $P$  and an increase of volume  $\Delta V > 0$  at low  $P$  (Fig. 3), while the  $T$ -denaturation by a positive entropy variation  $\Delta S > 0$  at high  $T$  and an *entropic penalty*  $\Delta S < 0$  at low  $T$  (Fig. 3). By varying the parameters  $v_{\text{HB}}^{(\Phi)}$  and  $J_{\Phi}$  we find that the first is relevant for the  $P$ -denaturation, as expected because it dominates Eq. (4), while the second affects the stability range in  $T$ . Both combine in a non-trivial way to regulate the low- $T$  entropic penalty.

Next, we study the case of a protein model with hydrophobic ( $\Phi$ ) and hydrophilic ( $\zeta$ ) residues [56, 12], with a residue-residue interaction matrix  $A_{i,j} = \epsilon_{\text{rr}}$  if residues  $i$  and  $j$  are n.n. in the unique native state, 0 otherwise. Water molecules interact with energy  $\epsilon_{\text{w},\Phi} < J$  and  $\epsilon_{\text{w},\zeta} > J$  with n.n.  $\Phi$  and  $\zeta$  residues respectively, accounting for the polarization of the solvent near the  $\zeta$  residues. The polar  $\zeta$  residues

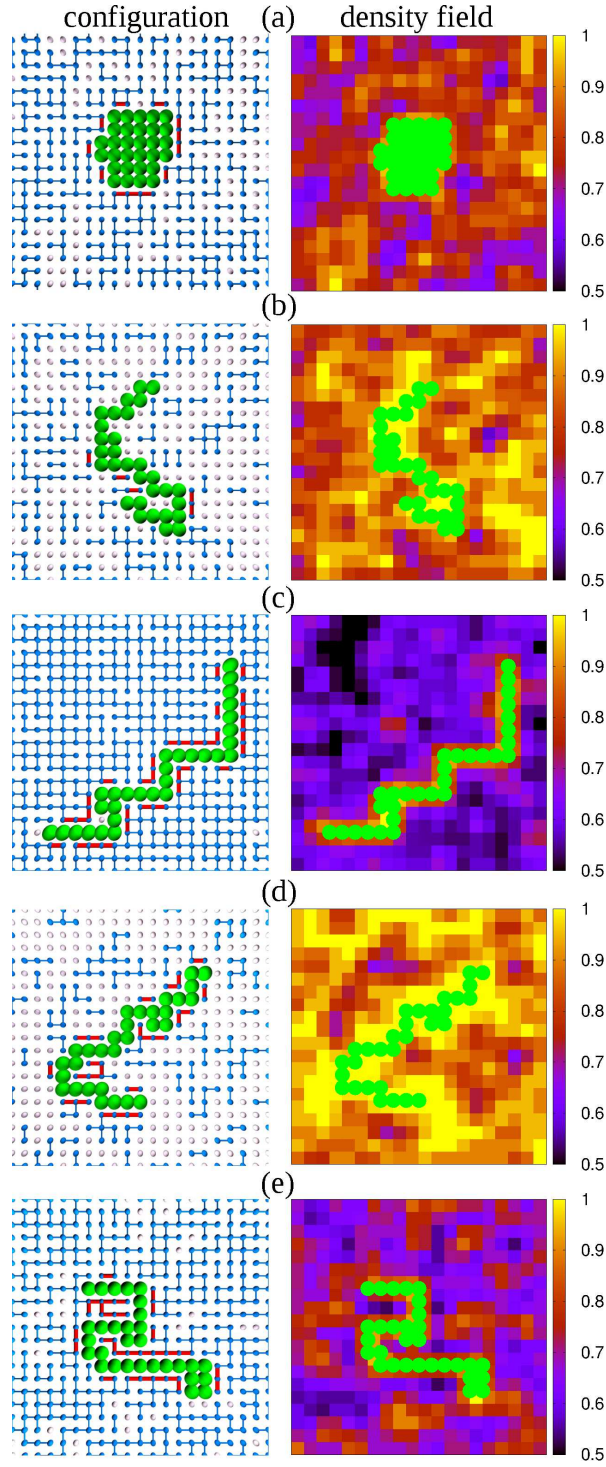


Figure 2: Typical configurations of a hydrated protein made of 30 residues (in green): (a) folded at the state point  $(Tk_B/4\epsilon, Pv_0/4\epsilon) = (0.25, 0.1)$  and unfolded (b) at high- $T$   $(0.9, 0.1)$ ; (c) at low- $T$   $(0.1, 0.1)$ ; (d) at high- $P$   $(0.25, 0.6)$ ; (e) at low- $P$   $(0.25, -0.3)$ . Left panels: Water molecules with/without HBs are represented in blue/white and bulk/interfacial HBs in blue/red. Right panels: Color coded water density field (from black for lower  $\rho$  to yellow for higher  $\rho$ ) calculated as  $v_0\rho_i^{(\lambda)} \equiv v_0/(v_0 + n_{\text{HB},i}^{(\lambda)}v_{\text{HB}}^{(\lambda)})$  where  $\lambda = \text{b}, \Phi$ , and  $n_{\text{HB},i}^{(\lambda)}$  is the number of HBs associated to the water molecule  $i$ , with  $\sum_i n_{\text{HB},i}^{(\lambda)} = N_{\text{HB}}^{(\lambda)}$ .



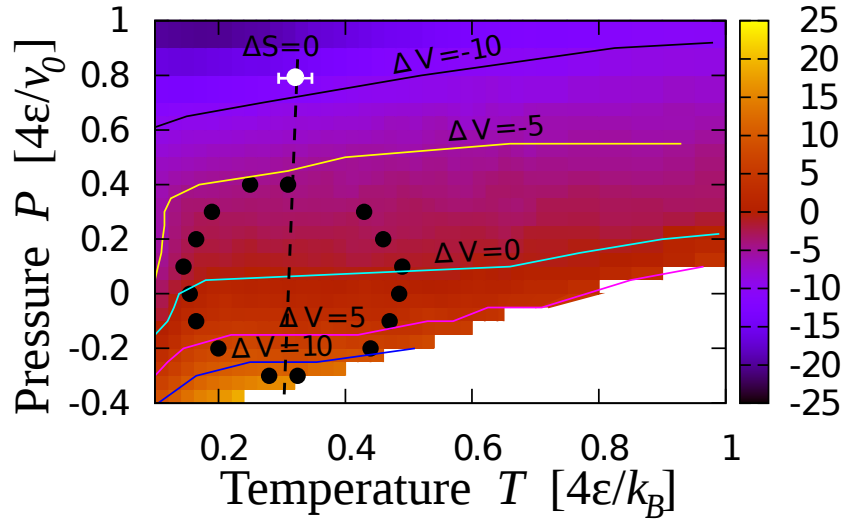


Figure 3: Volume change for the  $f \rightarrow u$  process in the  $T - P$  plane. Color coded volume change  $\Delta V$  (from black for largely negative to yellow for largely positive, in units of  $v_0$ ). Solid lines connect state points with constant  $\Delta V$ . Black points mark the SR. The locus  $\Delta V = 0$  has a positive slope and intersects the SR at the turning points with  $dT/dP|_{\text{SR}} = 0$ . The dashed line, connecting the points with  $dP/dT|_{\text{SR}} = 0$ , corresponds to the locus where  $\Delta S = 0$  and separates state points with  $\Delta S > 0$  (high  $T$ ) from those with  $\Delta S < 0$  (low  $T$ ) at the  $f \rightarrow u$  process. The white symbol marks the error in the dashed-line slope estimate.

distort the HB network of the surrounding water molecules, disrupting the local tetrahedral order. As a consequence we assume that a water molecules  $i$  forms a HB with the  $\zeta$  residue when its  $\sigma_{i,j}$  has the state  $q_j^{(\zeta)} = 1, \dots, q$  preassigned to the n.n.  $\zeta$  residue  $j$ . Finally, we consider that water-water enthalpy in the hydration shell is  $H_{\lambda,\lambda} \equiv -J_\lambda + P v_{\text{HB}}^{(\lambda)}$ , if both molecules are n.n. to the same type of residue or  $H_{\lambda,\mu} \equiv (H_{\lambda,\lambda} + H_{\mu,\mu})/2$  if the n.n. residues belong to different types, with  $\lambda, \mu = \Phi, \zeta$ , and  $J_\zeta \leq J$  [57] (Fig. 4).

Despite the complexity of the heteropolymer model, including residue-residue and water-residue interactions, our results are qualitatively similar to the previous for the simpler homopolymer model. This comparison suggests that the water contribution is relevant to the  $f \leftrightarrow u$  process for both the hetero- and the homopolymer case.

In conclusion, our model for protein folding reproduces the entire protein SR in explicit solvent and allows us to identify how water contributes to the  $T$ - and  $P$ -denaturation processes. The model is thermodynamically consistent with Hawleys theory but, in addition, allows for intermediate states for the  $f \leftrightarrow u$  process. We find that cold denaturation is energy-driven, while unfolding by pressurization and depressurization are density- and enthalpy-driven, respectively. For these mechanisms is essential to take into account how the water-water interaction and the water density change in the hydration shell. In particular, both properties control the low- $T$  entropic penalty. Our results are qualitatively robust against modification of the model parameters, within physical ranges, and the model is computationally efficient thanks to the adoption of a CG water model, representing a step towards the development of a theoretical and computational approach for protein design and engineering.

We thank Paolo Malgaretti, Marco Bernabei, Emanuele Locatelli, Ivan Coluzza, Carina Karner and Neus Patges for helpful discussions, and Spanish MEC FIS2012-31025 and EU FP7 NMP4-SL-2011-266737 grants for support. V.B. acknowledges support from Catalan grant FI-DGR 2010 and Italian “Angelo della Riccia” foundation.

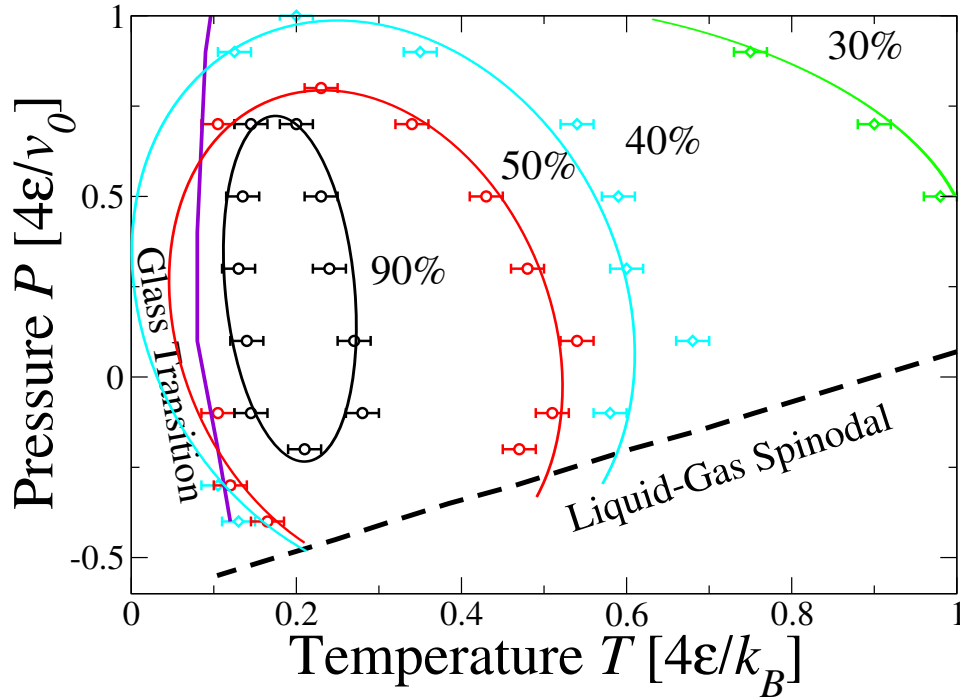


Figure 4: The SR for the heteropolymer with a unique native state is qualitatively similar to the SR in Fig. 1 for the homopolymer. We set  $\epsilon_{\text{rr}}/J = 0.7$ ,  $\epsilon_{\text{w},\Phi} = 0$ ,  $\epsilon_{\text{w},\zeta}/J = 1.17$ ,  $J_{\Phi}/J = 1.3$ ,  $J_{\zeta}/J = 0.5$ ,  $v_{\text{HB}}^{(\zeta)} = 0$ , with all the other parameters as in Fig. 1. We tested that changing the parameters, within physical ranges, modifies the SR, reproducing a variety of experimental SRs [11], but preserving the elliptic shape.

## References

- [1] Y. Levy and J. N. Onuchic, *Annu. Rev. Biophys. Biomol. Struct.* **35**, 389 (2006).
- [2] M. Kinoshita, *Int. J. Mol. Sci.* **10**, 1064 (2009).
- [3] R. Ravindra and R. Winter, *ChemPhysChem* **4**, 359 (2003).
- [4] A. Pastore, S. R. Martin, A. Politou, K. C. Kondapalli, T. Stemmler, and P. A. Temussi, *J. Am. Chem. Soc.* **129**, 5374 (2007).
- [5] F. Meersman, K. Smeller L. Heremans, *High Press. Res. An Int. J.* **19**, 263 (2000).
- [6] G. Hummer, S. Garde, A. E. García, M. E. Paulaitis, and L. R. Pratt, *Proc. Natl. Acad. Sci.* **95**, 1552 (1998).
- [7] F. Meersman, C. M. Dobson, and K. Heremans, *Chem. Soc. Rev.* **35**, 908 (2006).
- [8] N. V. Nucci, B. Fuglestad, E. A. Athanasoula, and A. J. Wand, *Proc. Natl. Acad. Sci.* **111**, 13846 (2014).
- [9] R. Wuttke, H. Hofmann, D. Nettels, M. B. Borgia, J. Mittal, R. B. Best, and B. Schuler, *Proc. Natl. Acad. Sci.* **111**, 5213 (2014).
- [10] S. A. Hawley, *Biochem.* **10**, 2436 (1971).
- [11] L. Smeller, *Biochim. Biophys. Acta* **1595**, 11 (2002).
- [12] P. De Los Rios and G. Caldarelli, *Phys. Rev. E* **62**, 8449 (2000).
- [13] C.-J. Tsai, J. V. Maizel, and R. Nussinov, *Crit. Rev. Biochem. Mol. Biol.* **37**, 55 (2002).
- [14] D. Paschek, S. Nonn, and A. Geiger, *Phys. Chem. Chem. Phys.* **7**, 2780 (2005).
- [15] M.I. Marqués, J.M. Borreguero, H.E. Stanley, and N. V. Dokholyan, *Phys. Rev. Lett.* **91**, 138103 (2003).
- [16] B. A. Patel, P. G. Debenedetti, F. H. Stillinger, and P. J. Rossky, *Biophys J* **93**, 4116 (2007).
- [17] M. V. Athawale, G. Goel, T. Ghosh, T. M. Truskett, and S. Garde, *Proc. Natl. Acad. Sci.* **104**, 733 (2007).
- [18] C. L. Dias, T. Ala-Nissila, M. Karttunen, I. Vattulainen, and M. Grant, *Phys. Rev. Lett.* **100**, 118101 (2008).
- [19] D. Nettels, S. Müller-Späth, F. Küster, H. Hofmann, D. Haenni, S. Rügger, L. Reymond, A. Hoffmann, J. Kubelka, B. Heinz, K. Gast, R. B. Best, and B. Schuler, *Proc. Natl. Acad. Sci.* **106**, 20740 (2009).
- [20] R. B. Best and J. Mittal, *The J. Phys. Chem. B* **114**, 14916 (2010).
- [21] S. N. Jamadagni, C. Bosoy, and S. Garde, *The J. Phys. Chem. B* **114**, 13282 (2010).
- [22] A. V. Badasyan, S. A. Tonoyan, Y. S. Mamasakhlov, A. Giacometti, A. S. Benight, and V. F. Morozov, *Phys. Rev. E* **83**, 051903 (2011).
- [23] S. Matysiak, P. G. Debenedetti, and P. J. Rossky, *The J. Phys. Chem. B* **116**, 8095 (2012).
- [24] T. Sumi and H. Sekino, *Phys. Chem. Chem. Phys.* **13**, 15829 (2011).
- [25] I. Coluzza, *PLoS ONE* **6**, e20853 (2011).
- [26] P. Das and S. Matysiak, *The J. Phys. Chem. B* **116**, 5342 (2012).



- [27] R. Sarma and S. Paul, *Chem. Phys.* **407**, 115 (2012).
- [28] A. Fernandez, *The J. Chem. Phys.* **139**, 085101 (2013).
- [29] G. Franzese and V. Bianco, *Food Biophys.* **8**, 153 (2013).
- [30] S. Abeln, M. Vendruscolo, C. M. Dobson, and D. Frenkel, *PLoS ONE* **9**, e85185 (2014).
- [31] A. Ben-Naim, *Eur. Phys. J. Spec. Top.* **223**, 927 (2014).
- [32] N. Muller, *Accounts Chem. Res.* **23**, 23 (1990).
- [33] G. Franzese, M. I. Marqués, and H. E. Stanley, *Phys. Rev. E* **67**, 011103 (2003).
- [34] K. Stokely, M. G. Mazza, H. E. Stanley, and G. Franzese, *Proc. Natl. Acad. Sci.* **107**, 1301 (2010).
- [35] M. G. Mazza, K. Stokely, S. E. Pagnotta, F. Bruni, H. E. Stanley, and G. Franzese, *Proc. Natl. Acad. Sci.* **108**, 19873 (2011).
- [36] F. de los Santos and G. Franzese, *J. Phys. Chem. B* **115**, 14311 (2011).
- [37] V. Bianco and G. Franzese, *Sci. Rep.* **4**, 4440 (2014).
- [38] A good parametrization for pure water is  $J/4\epsilon = 0.5$  and  $J_\sigma/4\epsilon = 0.05$  [34]. However, the presence of ions would result in the same modification of bulk water phase diagram [D. Corradini and P. Gallo, *J. Chem. Phys. B* **115**, 14161 (2011)] as decreasing  $J/J_\sigma$  in the many-body water model. Hence, here we fix  $J_\sigma$  and decrease  $J$  to account, qualitatively, for the ions in our protein solution.
- [39] L. Hernández de la Peña and P. G. Kusalik, *J. Am. Chem. Soc.* **127**, 5246 (2005).
- [40] A. K. Soper and M. A. Ricci, *Phys. Rev. Lett.* **84**, 2881 (2000).
- [41] C. Petersen, K.-J. Tielrooij, and H. J. Bakker, *The J. Chem. Phys.* **130**, 214511 (2009).
- [42] Y. Tarasevich, *Colloid J.* **73**, 257 (2011).
- [43] J. G. Davis, K. P. Gierszal, P. Wang, and D. Ben-Amotz, *Nat.* **491**, 582 (2012).
- [44] S. Sarupria and S. Garde, *Phys. Rev. Lett.* **103**, 037803 (2009).
- [45] V. Bianco, S. Iskov, and G. Franzese, *J. Biol. Phys.* **38**, 27 (2012).
- [46] K. Lum, D. Chandler, and J. D. Weeks, *The J. Phys. Chem. B* **103**, 4570 (1999).
- [47] D. Schwendel, T. Hayashi, R. Dahint, A. Pertsin, M. Grunze, R. Steitz, and F. Schreiber, *Langmuir* **19**, 2284 (2003).
- [48] T. R. Jensen, M. Østergaard Jensen, N. Reitzel, K. Balashev, G. H. Peters, K. Kjaer, and T. Bjørnholm, *Phys. Rev. Lett.* **90**, 086101 (2003).
- [49] D. A. Doshi, E. B. Watkins, J. N. Israelachvili, and J. Majewski, *Proc. Natl. Acad. Sci.* **102**, 9458 (2005).
- [50] R. Godawat, S. N. Jamadagni, and S. Garde, *Proc. Natl. Acad. Sci.* **106**, 15119 (2009).
- [51] V. M. Dadarlat and C. B. Post, *Biophys. J.* **91**, 4544 (2006).
- [52] E. G. Strelakova, J. Luo, H. E. Stanley, G. Franzese, and S. V. Buldyrev, *Phys. Rev. Lett.* **109**, 105701 (2012).
- [53] N. Giovambattista, P. J. Rossky, and P. G. Debenedetti, *Phys. Rev. E* **73**, 041604 (2006).

- [54] This approximation implies that our calculations are valid only for  $P < 1/k_1$  where the HB contribution to the isothermal compressibility of the  $\Phi$  hydration shell,  $K_T^{(\text{HB},\Phi)} \equiv -(1/V^{(\Phi)})(\partial V^{(\Phi)}/\partial P)_T \simeq (k_1/(1 - k_1P)) - (1/N_{\text{HB}}^{(\Phi)})(\partial N_{\text{HB}}^{(\Phi)}/\partial P)_T$  is finite.
- [55] S. V. Buldyrev, P. Kumar, P. G. Debenedetti, P. J. Rossky, and H. E. Stanley, Proc. Natl. Acad. Sci. **104**, 20177 (2007).
- [56] K. F. Lau and K. A. Dill, Macromol. **22**, 3986 (2002).
- [57] J.-X. Cheng, S. Pautot, D. A. Weitz, and X. S. Xie, Proc. Natl. Acad. Sci. **100**, 9826 (2003).